

An Empirical Study of the Collapsing Problem in Semi-Supervised 2D Human Pose Estimation

Rongchang Xie
Peking University
rongchangxie
@pku.edu.cn

Chunyu Wang
Microsoft Research Asia
chunuwa@microsoft.com

Wenjun Zeng
Microsoft Research Asia
wezeng@microsoft.com

Yizhou Wang
Peking University
yizhou.wang
@pku.edu.cn

Abstract

The state-of-the-art semi-supervised learning models are consistency-based which learn about unlabeled images by maximizing the similarity between different augmentations of an image. But when we apply the methods to human pose estimation which has extremely imbalanced class distribution, the models often collapse and predict every pixel in unlabeled images as background. This is because the decision boundary may pass through the high-density area of the minor class so more and more pixels are gradually misclassified as the background class. In this work, we present a surprisingly simple approach to drive the model to learn in the correct direction. For each image, it composes a pair of easy and hard augmentations and uses the more accurate predictions on the easy image to teach the network to learn about the hard one. The accuracy superiority of teaching signals allows the network to be “monotonically” improved which effectively avoids collapsing. We apply our method to recent pose estimators and find that they achieve significantly better performances than their supervised counterparts on three public datasets.

1. Introduction

Human pose estimation is a core problem in computer vision which has many applications such as 3D pose modeling [41, 31] and action recognition [33]. The performances on public datasets [1, 20] have been continuously improved in recent years [5, 27, 30] which is great for advancing human understanding. But there is a more important but less explored problem of learning robust models that perform well on unseen wild images. In general, there are two ways to achieve this ambitious goal. One is to fit the “whole” world by infinitely increasing the number of (unlabeled) training images. The other is to transfer pre-trained models to new domains by unsupervised finetuning. The common basis behind the two approaches is Semi-Supervised Learn-

ing (SSL)— how to leverage unlabeled images to obtain a generalizable model?

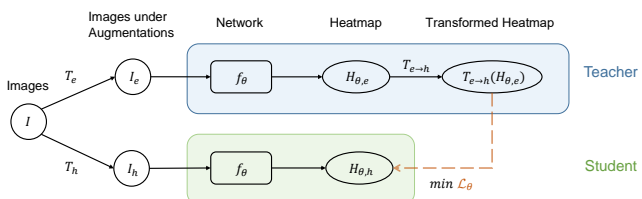


Figure 1. Our approach to avoid collapsing in semi-supervised human pose estimation. For each unlabeled image, we compose an easy and hard image pair I_e and I_h using two augmentation methods T_e and T_h , respectively, and feed them to the network f_θ . We use the heatmaps $T_{e \rightarrow h}(\mathbf{H}_{\theta,e})$ on the easy image to teach the network to learn about the hard image. $T_{e \rightarrow h}$ maps the two heatmaps of the augmented images. \mathcal{L}_θ represents the consistency loss. The accuracy superiority allows the network to be “monotonically” improved which avoids collapsing.

The previous SSL works have primarily focused on the classification task. In general, there are two strategies to explore unlabeled images. The first is Pseudo labeling [23, 36] which first learns an initial model on only labeled images in a supervised way. Then, for each unlabeled image, it applies the initial model to obtain hard or soft pseudo labels representing its category. Finally, it learns the ultimate model on the combined dataset of labeled and pseudo-labeled images. However, the performance of the method is largely limited by that of the initial model which is learned only on the labeled images and fixed thereafter.

The second class of methods [2, 17, 24, 25, 28] learn about unlabeled images by requiring the network to have similar predictions for different augmentations of the same image. They have advantages over the pseudo labeling methods because their performances are not limited by that of the fixed labeling network. However, when we try to apply them to 2D pose estimation in our experiments, we find that all of them encounter the collapsing problem meaning that, within few training iterations, the models begin to pre-

dict every pixel in unlabeled images as background. As a result, they not only fail to learn anything from unlabeled images but also the performances are even worse than the initial supervised model.

An Empirical Study of the Collapsing Problem in Semi-Supervised 2D Human Pose Estimation

The collapsing problem is not identified as a serious issue in previous works because most of them were only evaluated on the well-balanced classification task. But we find it is vital for tasks with severe class imbalance such as human pose estimation, which has not received sufficient attention. It occurs because when the network makes different predictions on the corresponding pixels, it lacks sufficient information to determine the correct optimization path. Blindly minimizing their discrepancy causes the decision boundary to be incorrectly formed due to imbalance and pass through the high-density area of the minor class as revealed in [11]. It leads to the situation where a growing number of pixels are mis-classified as background.

The state-of-the-art semi-supervised learning models are consistency-based simple approach on unlabeled images by maximizing a similarity between different augmentations of each hard augmentation pair and, by definition, a network should obtain better accuracy on a certain dataset with easy models than on the same dataset with hard augmentation. Then, for each unlabeled image, we compose an easy and a hard augmentation, feed them to the network and obtain two heatmap predictions. We use the accurate predictions on the easy augmentation to teach the network to learn about the correct response to hard augmentation (see Figure 1). However, the hard augmentation will not be used for teaching the network to learn about the easy augmentation, which avoids high response samples being pulled to background. The accuracy superiority of teaching accurate responses of the teaching signals allows the network to be monotonically improved which stabilizes the training and avoids collapsing. We apply our method to the training pose estimation and find that they achieve significant improvement and applies to most consistency-based SSL methods such as [14, 17] for stopping collapsing. We empirically validate it on a simple baseline as well as on the state-of-the-art method [14] which jointly learns two models. Both methods collapse in their original setting and our easy-hard augmentation strategy helps avoid the problem. We systematically analyze a problem on imbalanced datasets with COCO and AP-101 and HR36N [13] with the unlabeled images as background. The proposed method on the unlabeled images have been continuously improved independently to the SuperPose [36] which has only a single unlabeled dataset for training. But as a comparison, the proposed method explores the benefit of learning both easy and hard augmentation methods to learn about the hard augmentation. The proposed method achieves the state-of-the-art pose estimation on the unlabeled dataset by finally increasing the number of unlabeled training images. Then, the proposed method achieves the state-of-the-art pose estimation on the unlabeled dataset by finally increasing the number of unlabeled training images. Then, the proposed method achieves the state-of-the-art pose estimation on the unlabeled dataset by finally increasing the number of unlabeled training images.

1. Introduction

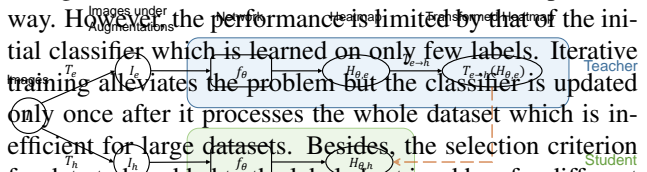
Both methods collapse in their original setting and our easy-hard augmentation strategy helps avoid the problem. We systematically analyze a problem on imbalanced datasets with COCO and AP-101 and HR36N [13] with the unlabeled images as background. The proposed method on the unlabeled images have been continuously improved independently to the SuperPose [36] which has only a single unlabeled dataset for training. But as a comparison, the proposed method explores the benefit of learning both easy and hard augmentation methods to learn about the hard augmentation. The proposed method achieves the state-of-the-art pose estimation on the unlabeled dataset by finally increasing the number of unlabeled training images. Then, the proposed method achieves the state-of-the-art pose estimation on the unlabeled dataset by finally increasing the number of unlabeled training images.

The versatile practical applications in various settings validate the values of this work.

SSL has been studied for a long time and most methods were evaluated for the classification task. In the following, we will discuss some of the recent works which incorporate deep learning. Our target is to provide a comprehensive review. Please refer to other survey papers such as [32] for a more comprehensive review.

Pseudo labeling [18, 23, 36, 37] is commonly used in SSL. The basic idea is to first learn an initial model on labeled images and then apply it to unlabeled images to estimate pseudo labels. The images with high confidence pseudo labels are added to the labeled dataset. Finally, it trains a stronger classifier on the extended dataset in a supervised way. However, the performance is limited by that of the initial classifier which is learned on only few labels. Iterative training alleviates the problem but the classifier is updated only once after it processes the whole dataset which is inefficient for large datasets. Besides, the selection criterion for data to be added to the labeled set is ad hoc for different tasks. For example, it is usually determined by prediction confidence which is not a reliable indicator. In this paper, we propose a novel method to avoid collapsing in semi-supervised learning. Our approach is to use unlabeled images calibrated with prediction accuracy in pose estimation. We compose an easy and a hard augmentation method. More recent SSL methods use the network to learn consistency loss [14, 17, 28, 29]. For example, the model [17] takes the history predictions on the unlabeled images and requires the consistency of the augmented images with them. The consistency loss will be more tolerant to incorrect labels but is "meretricious" when learning large datasets since history predictions change only once per epoch. Tarvainen et al. [28] present the mean teacher method which works better in the classification task.

The previous SSL works have primarily focused on the classification task. In general, there are two strategies to explore unlabeled images. The first is Pseudo labeling [33, 36] which first learns an initial model on only labeled images in a supervised way. Then, for each unlabeled image, it applies the initial model to obtain hard or soft pseudo labels representing its category. Finally, it learns the ultimate model on the combined dataset of labeled and pseudo labeled images. However, the performance of the method is largely limited by that of the initial model which is learned only on the labeled images and fixed thereafter. The second strategy is to identify labeled images by the quality of the network and provide similar predictions for different augmentations. The existing SSL methods have been designed for pose estimation. In labeling methods, because the disorder representation of joints, the that of the pseudo labeling task and provide a rigorous evaluation of the performance of this is a simple and practical method than that. We will release the code and hope that the models begin to pre-



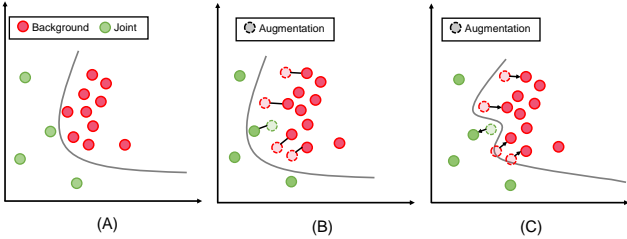


Figure 4. (A) the decision boundary before SSL. (B) background pixels are gradually pulled to the background class. (C) more accurate predictions of easy augmentation pull those background pixels back to the background class.

The state-of-the-art semi-supervised learning models are

3.1 Avoid Collapsing

The task of 2D pose estimation aims to detect locations of body joints in an image. We first introduce the concept of **collapsing**, which refers to the situation where the model predicts a joint location as background pixels. This is often caused by the model's inability to distinguish between background and joint pixels. In this case, the decision boundary is less likely to be incorrect. In our method, more accurate predictions of easy augmentation pull those background pixels back to the background class. This response sampling is pulled to the background class as a growing number of pixels are mis-classified as background.

3.2 The Collapsing Problem

Figure 5. Left: Average precision of a network on a dataset under different augmentation pairs and their effects on avoiding collapsing. “JC 5” represents Joint Cutout Augmentation on five joints (a novel hard augmentation method we introduce in Section 4.1). “RA 20” represents Random Augmentation [6].

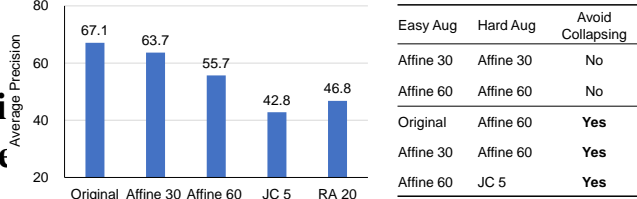


Figure 5. Left: Average precision of a network on a dataset under different augmentation pairs and their effects on avoiding collapsing. “JC 5” represents Joint Cutout Augmentation on five joints (a novel hard augmentation method we introduce in Section 4.1). “RA 20” represents Random Augmentation [6].

Figure 5. Top: results of the standard learn an initial model on labeled images, and then apply it to unlabeled images. Bottom: results of the proposed method on unlabeled images.

4. Implementation Details

4.1 Easy Hard Augmentation

The basic idea is to first learn an initial model on labeled images, and then apply it to unlabeled images. The proposed method consists of two parts: a standard supervised learning phase and a self-supervised learning phase.

4.2 The Collapsing Problem

Figure 6. Top: results of the standard learn an initial model on labeled images, and then apply it to unlabeled images. Bottom: results of the proposed method on unlabeled images.

4.3 The Collapsing Problem

Figure 7. Top: results of the standard learn an initial model on labeled images, and then apply it to unlabeled images. Bottom: results of the proposed method on unlabeled images.

4.4 The Collapsing Problem

Figure 8. Top: results of the standard learn an initial model on labeled images, and then apply it to unlabeled images. Bottom: results of the proposed method on unlabeled images.

4.5 The Collapsing Problem

Figure 9. Top: results of the standard learn an initial model on labeled images, and then apply it to unlabeled images. Bottom: results of the proposed method on unlabeled images.

4.6 The Collapsing Problem

Figure 10. Top: results of the standard learn an initial model on labeled images, and then apply it to unlabeled images. Bottom: results of the proposed method on unlabeled images.

4.7 The Collapsing Problem

Figure 11. Top: results of the standard learn an initial model on labeled images, and then apply it to unlabeled images. Bottom: results of the proposed method on unlabeled images.

4.8 The Collapsing Problem

Figure 12. Top: results of the standard learn an initial model on labeled images, and then apply it to unlabeled images. Bottom: results of the proposed method on unlabeled images.

4.9 The Collapsing Problem

Figure 13. Top: results of the standard learn an initial model on labeled images, and then apply it to unlabeled images. Bottom: results of the proposed method on unlabeled images.

4.10 The Collapsing Problem

Figure 14. Top: results of the standard learn an initial model on labeled images, and then apply it to unlabeled images. Bottom: results of the proposed method on unlabeled images.

4.11 The Collapsing Problem

Figure 15. Top: results of the standard learn an initial model on labeled images, and then apply it to unlabeled images. Bottom: results of the proposed method on unlabeled images.

4.12 The Collapsing Problem

Figure 16. Top: results of the standard learn an initial model on labeled images, and then apply it to unlabeled images. Bottom: results of the proposed method on unlabeled images.

4.13 The Collapsing Problem

Figure 17. Top: results of the standard learn an initial model on labeled images, and then apply it to unlabeled images. Bottom: results of the proposed method on unlabeled images.

4.14 The Collapsing Problem

Figure 18. Top: results of the standard learn an initial model on labeled images, and then apply it to unlabeled images. Bottom: results of the proposed method on unlabeled images.

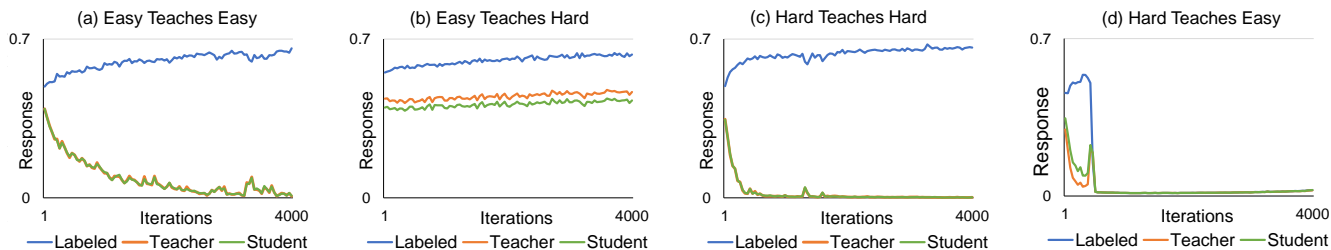


Figure 1 shows the training curves for different augmentation strategies. The blue line represents the results on labeled images and unlabeled images. The orange line represents the results on teacher's supervision and unlabeled images. The green line represents the results on student's supervision and unlabeled images. The x-axis is Iterations (1 to 4000) and the y-axis is Response (0 to 0.7).

Table 1: Performance of different augmentation strategies. The table shows the performance of different augmentation strategies on labeled and unlabeled images. The x-axis is the augmentation strategy and the y-axis is the performance. The values are the average response and the average precision (AP).

Table 2: Performance of different augmentation strategies. The table shows the performance of different augmentation strategies on labeled and unlabeled images. The x-axis is the augmentation strategy and the y-axis is the performance. The values are the average response and the average precision (AP).

Table 3: Performance of different augmentation strategies. The table shows the performance of different augmentation strategies on labeled and unlabeled images. The x-axis is the augmentation strategy and the y-axis is the performance. The values are the average response and the average precision (AP).

Table 4: Performance of different augmentation strategies. The table shows the performance of different augmentation strategies on labeled and unlabeled images. The x-axis is the augmentation strategy and the y-axis is the performance. The values are the average response and the average precision (AP).

Figure 2 shows the training curves for different augmentation strategies. The blue line represents the results on labeled images and unlabeled images. The orange line represents the results on teacher's supervision and unlabeled images. The green line represents the results on student's supervision and unlabeled images. The x-axis is Iterations (1 to 4000) and the y-axis is Response (0 to 0.7).

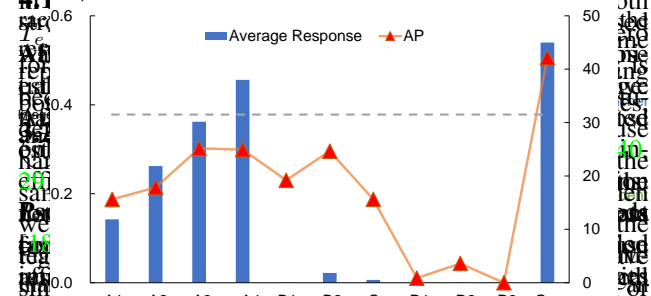


Figure 3 shows the training curves for different augmentation strategies. The blue line represents the results on labeled images and unlabeled images. The orange line represents the results on teacher's supervision and unlabeled images. The green line represents the results on student's supervision and unlabeled images. The x-axis is Iterations (1 to 4000) and the y-axis is Response (0 to 0.7).

Figure 4 shows the training curves for different augmentation strategies. The blue line represents the results on labeled images and unlabeled images. The orange line represents the results on teacher's supervision and unlabeled images. The green line represents the results on student's supervision and unlabeled images. The x-axis is Iterations (1 to 4000) and the y-axis is Response (0 to 0.7).

References

- [1] The COCO TEST set is the state-of-the-art analysis of the COCO TEST. The COCO Train set is the dataset description. COCO WILD set is the unlabeled set. The person detection results are provided by Simple Baseline [35] and flipping strategy is used.
- [2] Zhanchen Ke, Daoye Wang, Qiong Yan, Jimmy Ren, and Keyson WH Lim. Final student: Breaking the limits of the teacher in semi-supervised learning. *Proceedings of the IEEE International Conference on Computer Vision*, pages 6736–6736, 2019.
- [3] Peter Gao, Yifan Peng, and Peter Gao. A new benchmark and state of the art analysis. In *Proceedings of the IEEE Conference on Computer Vision and Pattern Recognition*, pages 329–329, 2014.
- [4] ResNet-50. 384 × 288. 58.7. 71.9.
- [5] ResNet-50. 384 × 288. 58.7. 71.9.
- [6] ResNet-50. 384 × 288. 58.7. 71.9.
- [7] ResNet-50. 384 × 288. 58.7. 71.9.
- [8] ResNet-50. 384 × 288. 58.7. 71.9.
- [9] ResNet-50. 384 × 288. 58.7. 71.9.
- [10] ResNet-50. 384 × 288. 58.7. 71.9.
- [11] ResNet-50. 384 × 288. 58.7. 71.9.
- [12] ResNet-50. 384 × 288. 58.7. 71.9.
- [13] ResNet-50. 384 × 288. 58.7. 71.9.
- [14] ResNet-50. 384 × 288. 58.7. 71.9.
- [15] ResNet-50. 384 × 288. 58.7. 71.9.
- [16] ResNet-50. 384 × 288. 58.7. 71.9.
- [17] ResNet-50. 384 × 288. 58.7. 71.9.
- [18] ResNet-50. 384 × 288. 58.7. 71.9.
- [19] ResNet-50. 384 × 288. 58.7. 71.9.
- [20] ResNet-50. 384 × 288. 58.7. 71.9.
- [21] ResNet-50. 384 × 288. 58.7. 71.9.
- [22] ResNet-50. 384 × 288. 58.7. 71.9.
- [23] ResNet-50. 384 × 288. 58.7. 71.9.
- [24] ResNet-50. 384 × 288. 58.7. 71.9.
- [25] ResNet-50. 384 × 288. 58.7. 71.9.
- [26] ResNet-50. 384 × 288. 58.7. 71.9.
- [27] ResNet-50. 384 × 288. 58.7. 71.9.
- [28] ResNet-50. 384 × 288. 58.7. 71.9.
- [29] ResNet-50. 384 × 288. 58.7. 71.9.
- [30] ResNet-50. 384 × 288. 58.7. 71.9.
- [31] ResNet-50. 384 × 288. 58.7. 71.9.
- [32] ResNet-50. 384 × 288. 58.7. 71.9.
- [33] ResNet-50. 384 × 288. 58.7. 71.9.
- [34] ResNet-50. 384 × 288. 58.7. 71.9.
- [35] ResNet-50. 384 × 288. 58.7. 71.9.
- [36] ResNet-50. 384 × 288. 58.7. 71.9.
- [37] ResNet-50. 384 × 288. 58.7. 71.9.
- [38] ResNet-50. 384 × 288. 58.7. 71.9.
- [39] ResNet-50. 384 × 288. 58.7. 71.9.
- [40] ResNet-50. 384 × 288. 58.7. 71.9.
- [41] ResNet-50. 384 × 288. 58.7. 71.9.
- [42] ResNet-50. 384 × 288. 58.7. 71.9.
- [43] ResNet-50. 384 × 288. 58.7. 71.9.
- [44] ResNet-50. 384 × 288. 58.7. 71.9.
- [45] ResNet-50. 384 × 288. 58.7. 71.9.
- [46] ResNet-50. 384 × 288. 58.7. 71.9.
- [47] ResNet-50. 384 × 288. 58.7. 71.9.
- [48] ResNet-50. 384 × 288. 58.7. 71.9.
- [49] ResNet-50. 384 × 288. 58.7. 71.9.
- [50] ResNet-50. 384 × 288. 58.7. 71.9.
- [51] ResNet-50. 384 × 288. 58.7. 71.9.
- [52] ResNet-50. 384 × 288. 58.7. 71.9.
- [53] ResNet-50. 384 × 288. 58.7. 71.9.
- [54] ResNet-50. 384 × 288. 58.7. 71.9.
- [55] ResNet-50. 384 × 288. 58.7. 71.9.
- [56] ResNet-50. 384 × 288. 58.7. 71.9.
- [57] ResNet-50. 384 × 288. 58.7. 71.9.
- [58] ResNet-50. 384 × 288. 58.7. 71.9.
- [59] ResNet-50. 384 × 288. 58.7. 71.9.
- [60] ResNet-50. 384 × 288. 58.7. 71.9.
- [61] ResNet-50. 384 × 288. 58.7. 71.9.
- [62] ResNet-50. 384 × 288. 58.7. 71.9.
- [63] ResNet-50. 384 × 288. 58.7. 71.9.
- [64] ResNet-50. 384 × 288. 58.7. 71.9.
- [65] ResNet-50. 384 × 288. 58.7. 71.9.
- [66] ResNet-50. 384 × 288. 58.7. 71.9.
- [67] ResNet-50. 384 × 288. 58.7. 71.9.
- [68] ResNet-50. 384 × 288. 58.7. 71.9.
- [69] ResNet-50. 384 × 288. 58.7. 71.9.
- [70] ResNet-50. 384 × 288. 58.7. 71.9.
- [71] ResNet-50. 384 × 288. 58.7. 71.9.
- [72] ResNet-50. 384 × 288. 58.7. 71.9.
- [73] ResNet-50. 384 × 288. 58.7. 71.9.
- [74] ResNet-50. 384 × 288. 58.7. 71.9.
- [75] ResNet-50. 384 × 288. 58.7. 71.9.
- [76] ResNet-50. 384 × 288. 58.7. 71.9.
- [77] ResNet-50. 384 × 288. 58.7. 71.9.
- [78] ResNet-50. 384 × 288. 58.7. 71.9.
- [79] ResNet-50. 384 × 288. 58.7. 71.9.
- [80] ResNet-50. 384 × 288. 58.7. 71.9.
- [81] ResNet-50. 384 × 288. 58.7. 71.9.
- [82] ResNet-50. 384 × 288. 58.7. 71.9.
- [83] ResNet-50. 384 × 288. 58.7. 71.9.
- [84] ResNet-50. 384 × 288. 58.7. 71.9.
- [85] ResNet-50. 384 × 288. 58.7. 71.9.
- [86] ResNet-50. 384 × 288. 58.7. 71.9.
- [87] ResNet-50. 384 × 288. 58.7. 71.9.
- [88] ResNet-50. 384 × 288. 58.7. 71.9.
- [89] ResNet-50. 384 × 288. 58.7. 71.9.
- [90] ResNet-50. 384 × 288. 58.7. 71.9.
- [91] ResNet-50. 384 × 288. 58.7. 71.9.
- [92] ResNet-50. 384 × 288. 58.7. 71.9.
- [93] ResNet-50. 384 × 288. 58.7. 71.9.
- [94] ResNet-50. 384 × 288. 58.7. 71.9.
- [95] ResNet-50. 384 × 288. 58.7. 71.9.
- [96] ResNet-50. 384 × 288. 58.7. 71.9.
- [97] ResNet-50. 384 × 288. 58.7. 71.9.
- [98] ResNet-50. 384 × 288. 58.7. 71.9.
- [99] ResNet-50. 384 × 288. 58.7. 71.9.
- [100] ResNet-50. 384 × 288. 58.7. 71.9.

References “Pattern recognition,” pages 569–570, 2019.

Response	Workshop	Topic	Score	Rank	Workshop	Topic	Score	Rank
[13]	Maximiliano Andrés, Leonid Bisk, Boris P. Gurevich, and Barak Shalev-Shanmug	Improving the Expressiveness of Parametric Models: When the Target is a Large-Scale Image and State of the Art Analysts. In <i>Proceedings of the IEEE Conference on Computer Vision and Pattern Recognition</i> , pages 68–76, 2019.	34.0	34.0	Arash Ghahramani, Robert I. Greis, and David M. Blei	Principles of Variational Autoencoders	77.0	77.0
	SBM Models: When the Target is a Large-Scale Image and State of the Art Analysts. In <i>Proceedings of the IEEE Conference on Computer Vision and Pattern Recognition</i> , pages 68–76, 2019.	68.6	68.6	Wenbin Dou, Yuhang Zhou, and Conference on Computer Vision and Pattern Recognition	77.7	77.7		
	HR: A Novel Hierarchical Representation for Image Classification. In <i>Proceedings of the IEEE Conference on Computer Vision and Pattern Recognition</i> , pages 68–76, 2019.	63.6	63.6	Federik P. Kingma and Diederik P. Kingma	77.7	77.7		

[illegible]

different local conditions, and the time and algorithms for the
e teachers' community and educational approaches among them. The
68.6 But, the findings from the research suggest that the
63.6 and the study has found that the research is not
63.6 research, but the research is not the same as the research

Figure 1: Comparison of the proposed method with the baseline methods. The proposed method (V2) achieves the highest accuracy (0.92) and the lowest error rate (0.08) among all methods. The baseline methods (V1, V3, V4, V5, V6, V7, V8, V9, V10, V11, V12, V13, V14, V15, V16, V17, V18, V19, V20, V21, V22, V23, V24, V25, V26, V27, V28, V29, V30, V31, V32, V33, V34, V35, V36, V37, V38, V39, V40, V41, V42, V43, V44, V45, V46, V47, V48, V49, V50, V51, V52, V53, V54, V55, V56, V57, V58, V59, V60, V61, V62, V63, V64, V65, V66, V67, V68, V69, V70, V71, V72, V73, V74, V75, V76, V77, V78, V79, V80, V81, V82, V83, V84, V85, V86, V87, V88, V89, V90, V91, V92, V93, V94, V95, V96, V97, V98, V99, V100) show lower accuracy and higher error rates. The proposed method (V2) is highlighted in red.

[illegible]

and Jian Sun. Rethinking on multi-stage networks for human pose estimation. *arXiv preprint arXiv:1901.00148*, 2019.

[illegible]

On September 11, 2001, the World Trade Center in New York City was attacked by two hijacked commercial airplanes. The attacks resulted in the deaths of nearly 3,000 people and caused billions of dollars in damage. The World Trade Center was a major symbol of American capitalism and globalization. The attacks were a major turning point in the history of the world, leading to the War on Terror and the invasion of Iraq and Afghanistan. The World Trade Center was a major symbol of American capitalism and globalization. The attacks were a major turning point in the history of the world, leading to the War on Terror and the invasion of Iraq and Afghanistan.

Figure 1 displays two side-by-side images of a document page, illustrating the results of the proposed refinement process. The left image shows the original bounding boxes (red, green, blue, and yellow) around the text. The right image shows the refined bounding boxes, which are more precise and better aligned with the text, demonstrating the effectiveness of the refinement process.

Using the same data, we can also create a confusion matrix. The confusion matrix is a table that shows the counts of data points that are correctly classified, incorrectly classified, or not classified at all. The confusion matrix is a useful tool for evaluating the performance of a classification model.

[18] <https://www.youtube.com/watch?v=20x0T0B8750>, 2020. <https://www.youtube.com/watch?v=20x0T0B8750>.
 [19] Holgeritz, James, Chloé Gossens-Barbier, Mladen Stokich, and Christian

[illegible]

157. [Liu, J. and G. Li. 2015. "Causal Inference in the Presence of Treatment Heterogeneity: Estimation and Selection." *Journal of the Royal Statistical Society B* 77\(4\): 1111-1154.](#)

Supplementary Material of An Empirical Study of the Collapsing Problem in Semi-Supervised 2D Human Pose Estimation

Anonymous ICCV submission

Paper ID 3910

A. Other Attempts to Avoid Collapsing

The *standard consistency-based method* (Described in Section 3.1 and 3.2) suffers from collapsing problem in 2D pose estimation. In this section, we also investigate the effects of other factors like the number of labeled examples, and unsupervised loss weight on the collapsing problem.

The following experiments show that adjusting these factors can *Not* fully solve the collapse problem. In all experiments, the response to the unlabeled sample always has a downward trend, and the final model accuracy is lower than the initial supervised model. It is worth noting that the augmentation parameters η and η' are sampled in the same distribution (See Section 3.1) in these experiments, and our easy-hard augmentation strategy is not involved.

A.1. Decrease Unsupervised Loss Weight λ

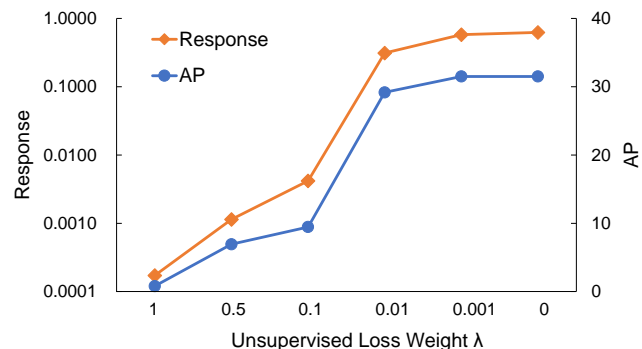


Figure 9. Effect of unsupervised loss weight λ . With small consistency coefficient, the response for unlabeled examples still decreases but in a relatively slow speed.

The coefficient λ controls the importance of consistency loss L_u . One possible opinion is that too large weight λ leads to the instability in training process. The effect of decreasing λ is shown in Figure 9. $\lambda = 1$ is the default setting and $\lambda = 0$ means that only supervised loss L_s is used. All of these are trained with the same number of epochs. The

result indicates that lower coefficient slightly reduce the degree of degradation but the degradation still happens. With different coefficient values, the response and AP are always worse than the supervised model.

A.2. Increase Labeled Examples

Labels	Response	AP	Supervised AP
COCO 1K	0.0002	0.8	31.5
COCO 5K	0.0023	13.0	46.4
COCO 10K	0.0105	26.2	51.1
COCO 150K (Full)	0.0122	46.8	67.1

Table 9. Increasing the labeled examples do Not address the collapsing problem. "Supervised AP" represents the supervised model using only labeled examples. Even with sufficient labels, the SSL training still degrades the performance compared to supervised model.

Another question is whether too few labels causes the collapsing. As is shown in Table 9, with the increase of labels, the validation performance has improved (From 0.8% to 46.8%). However, It did not fully solve the collapsing problem, as the response level is still low and performance is degraded. The results indicate that the even under a large number of labeled samples, consistency loss still drives the network to generate low-response heatmap for unlabeled examples, and finally degrade the generalization performance of model. In contrast, our method can significantly improve the performance regardless of the number of labeled examples.

B. Dual Networks

More details about dual networks, including the algorithm flow, the motivation and advantages, are provided in this part. In dual networks learning, we jointly learn two networks f_θ and f_ξ . We first train them separately on labeled images from different initialization. Then we jointly train them on both labeled and unlabeled images. The Fig-

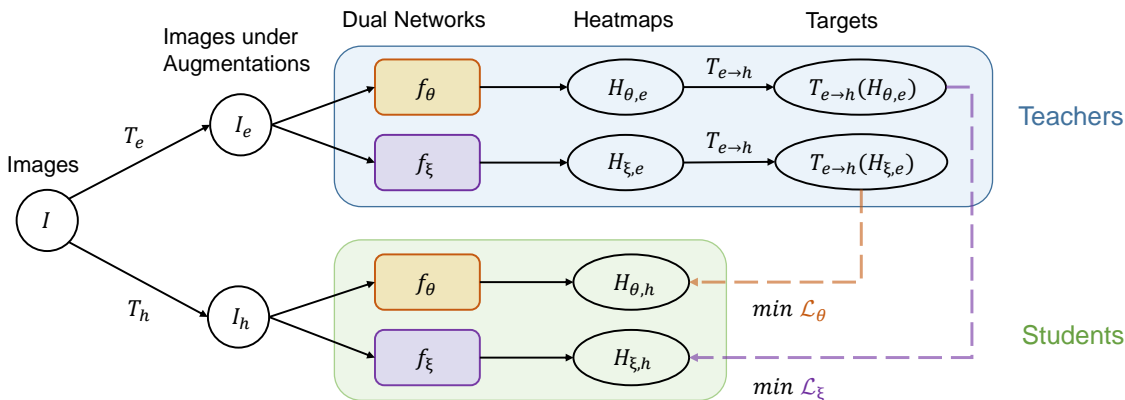


Figure 10. Framework of our Dual Networks Learning. Each of the two networks serves as both a teacher and a student. They take easy and hard images when they are teachers and students, respectively.

A. Other Attempts to Avoid Collapsing

Figure 10 demonstrates the framework of our method (dual network) and Algorithm 1 describes the algorithm process. In Section 3.1 and 3.2) suffers from collapsing problem in 2D pose estimation. In this section, we also investigate the effects of other factors like the number of labeled examples, and unsupervised loss weight on the collapsing problem. The following experiments show that adjusting these factors can not fully solve the collapse problem. In all experiments, the response to the unlabeled sample always has a downward trend, and the final model accuracy is lower than the initial supervised model. It is worth noting that the augmentation parameters η and η' are sampled in the same distribution (See Section 3.1) in these experiments, and our easy-hard augmentation strategy is not involved.

A.1. Decrease Unsupervised Loss Weight

Two models and boosts the final performance [?, ?]. (3) The two networks can be updated and improved at the same time, and no response will become the bottleneck. In fact, the accuracy of two networks are very similar after training if they use the same network structure.

C. Additional Experimental Results

C.1. Augmentation Hyper-Parameters

We study the effect of augmentation hyper-parameters in this part. The dual networks (with “easy-hard” augmentation method) is used as training method. The COCO 1K subset is used as labeled set and COCO TRAIN is used as Figure 9. Effect of unsupervised loss weight λ . With small consistency coefficient, the response for unlabeled examples still decreases but in a relatively slow speed. The best value of hyper-parameters is selected and used as the default setting.

The coefficient λ controls the importance of consistency. Joint Cutout possible question is that too large weight may lead to the instability in training. The effect of λ will increase this difficulty. Figure 11. We choose default setting $\lambda = 0.001$ to analyze the effect of hyper-parameters. The default parameters (Figure 11) with the same number of epochs, the first

result indicates that lower coefficient slightly reduce the degree of degradation but the degradation still happens. With different coefficient values, the response and AP are always worse than the supervised model.

Input: $\mathcal{L} = \{(I_i, H_i)\}_{i=1}^N$: Batch of labeled data.
Input: $\mathcal{U} = \{I_u\}_{u=1}^M$: Batch of unlabeled data.

Algorithm 1: Dual Networks Learning

Output: θ, ξ : Updated model parameters

Labels	Response	AP	Supervised AP
COCO 1K	0.0002	0.8	31.5
COCO 5K	0.0023	13.0	46.4
COCO 10K	0.0105	26.2	51.1
COCO 50K (Full)	0.0122	46.8	67.1

Table 1. Results of increasing the labeled examples do not address the collapsing problem. “Supervised AP” represents the supervised model using only labeled examples. Even with sufficient labels, the SSL training still degrades the performance compared to supervised model.

8. Another question is whether too few labels causes the collapsing problem. As shown in Table 1, with the increase of labels, the validation performance has improved (From 0.8% to 46.8%). However, it did not fully solve the collapsing problem, as the response level is still low and performance is degraded. The results indicate that the even under a large number of labeled samples, consistency loss still drives the network to generate low-response heatmap for unlabeled examples, and finally degrade the generalization performance of model. In contrast, our method can significantly improve the performance regardless of the number of labeled examples.

performance. Further increasing m can not boost accuracy, this is because the remaining image region is too small to have effective information for localization.

More details about dual networks, including the algorithm flow, the motivation and advantages, are provided in Band Augmental Networks studying the effect of the distortion network itself, and Band Augmental Networks augmentation on unlabeled images and randomly sampled labeled images are jointly. This figure shows labeled and unlabeled images. If 20. Fig

Supplementary Material of An Empirical Study of the Collapsing Problem in Semi-Supervised 2D Human Pose Estimation

Anonymous ICCV submission

Paper ID 3910

A. About Collapsing Problem

The *standard consistency-based method* (Described in Section 3.1 and 3.2) suffers from collapsing problem in 2D pose estimation. In this section, we first visualize the imbalanced distribution of heatmap value and show that the standard consistency method failed to predict the minority classes (Foreground). Then we also investigate the effects of other factors like the number of labeled examples, and unsupervised loss weight on the collapsing problem.

A.1. Imbalanced Distribution

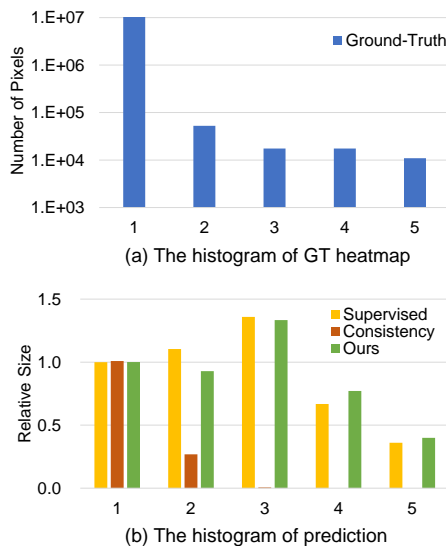


Figure 9. The value range of heatmap is divided into 5 bins, and the histogram is made according to the number of pixels. (a) The distribution of GT heatmap value is extremely imbalanced. (b) The relative size of prediction compared to GT heatmap. The number is counted in COCO validation set.

The standard heatmap encoding method is to generate a 2D gaussian kernel centred at the joint, which is imbalanced in pixel value naturally. As is shown in Figure 9(a),

we divide the value range of Ground-Truth (GT) heatmap $([0, 1])$ into 5 bins and plot the histogram. The number of low-value pixels greatly exceeds high-value pixels and the ratio is around 1000. In Figure 9 (b), the distribution of predicted heatmap in different method is shown. The relative size compared to the size GT heatmap is displayed for comparison. The standard consistency-based method without easy-hard augmentation further aggravated the imbalance problem. It failed to predict high-value pixels, which is consistent with the collapsing described earlier. Compared to it, our method avoids the collapse problem, and the distribution on different values is more reasonable.

A.2. Other Attempts to Avoid Collapsing

We try to adjust the factors like the number of labels, and unsupervised loss weight, but the results show that it can *Not* fully solve the collapse problem. In all experiments, the response to the unlabeled sample always has a downward trend, and the final model accuracy is lower than the initial supervised model. It is worth noting that the augmentation parameters η and η' are sampled in the same distribution (See Section 3.1) in these experiments, and our easy-hard augmentation strategy is not involved.

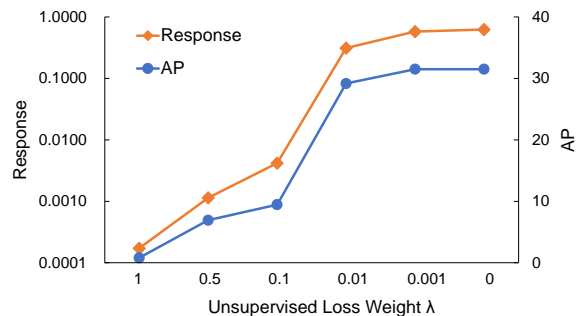


Figure 10. Effect of unsupervised loss weight λ . With small consistency coefficient, the response for unlabeled examples still decreases but in a relatively slow speed.

2

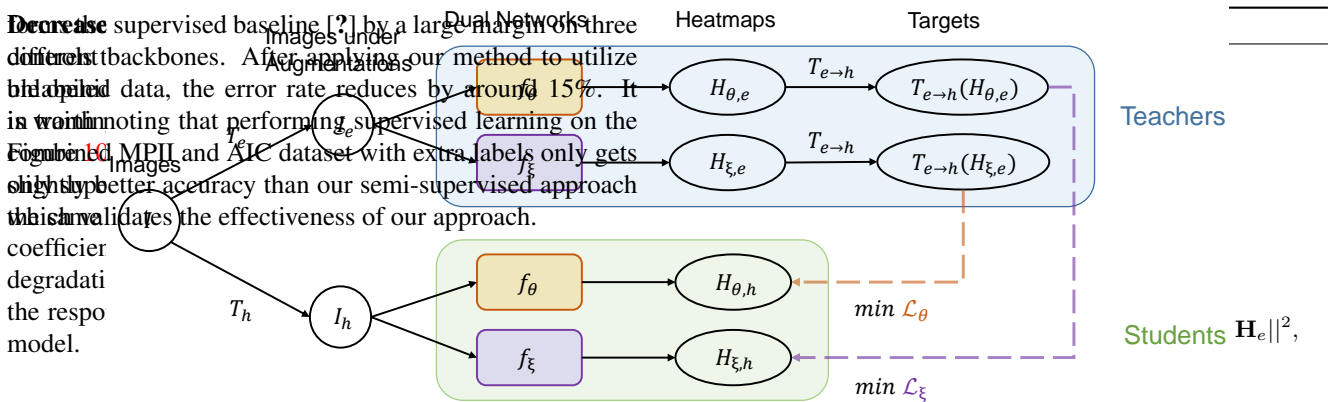
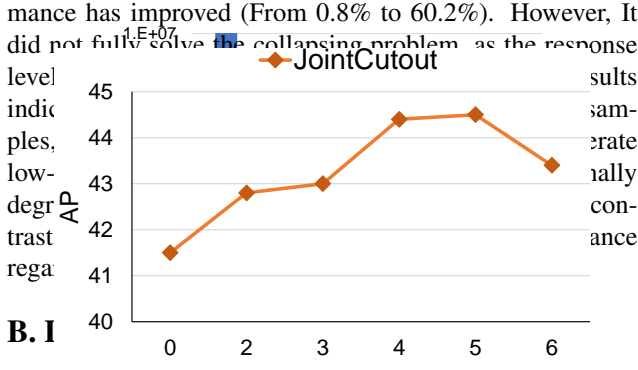


Figure 11. Framework of our Dual Networks Learning. Each of the two networks serves as both a teacher and a student. They take easy and hard images when they are teachers and students, respectively. Randomly sample augmentations η_e and η_h .

A. About Collapsing Problem

We compare a supervised baseline that is trained only on the majority class (Simple Baseline 1) with a supervised balanced method (Ours) that uses a supervised balanced distribution of heatmap value and show that the proposed method consistently outperforms the supervised baseline in terms of performance on the minority class (background). Then, we also investigate the effects of other factors like the number of labeled examples and unsupervised loss weight on the collapsing problem.

Adaptive Imbalanced Distribution ✓ 97.1
 whether too few labels causes the collapse. As is shown
 in Table 9, with the increase of labels, the validation perfor-
 mance increases. ✗ 97.4

[illegible][illegible]

A.2. Other Attempts to Avoid Collapsing

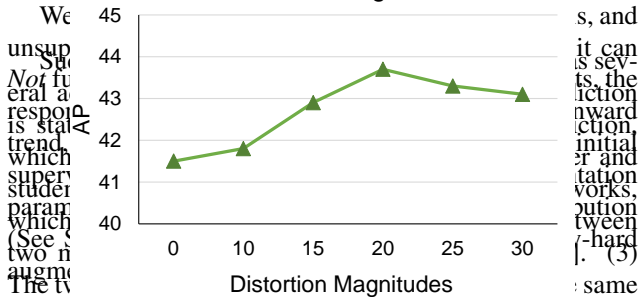


Figure 15: Effect of the distortion of magnitudes in RandAugment. The accuracy of two networks are very similar after training if they have the same network structure.

Rand Augment We also study the effect of the distortion magnitude α in RandAugment. Two augmentation trans-

C. Additional Experimental Results

C.4 Augmentation Hyper-Parameters

C.2. MPII Validation Dataset

We tested several methods (David, 2006) of VRA. The first used as a baseline the method of David (2006) and the second used as a baseline the method of Gumbel and Pearson (1999). The third used as a baseline the method of Gumbel and Pearson (1999) and the fourth used as a baseline the method of Gumbel and Pearson (1999).

data sets of information. Although socially, it does **not** show the trends but in a relatively slow and **stagnant** approach outper-

is successful in identifying misclassification, applying output-